Analysis of Hydride Transfer and Cofactor Fluorescence Decay in Mutants of Dihydrofolate Reductase: Possible Evidence for Participation of Enzyme Molecular Motions in Catalysis†

Martin F. Farnum,*,‡ Douglas Magde,*,‡ Elizabeth E. Howell,§ John T. Hirai,‡ Mark S. Warren,‡ Janet K. Grimsley,‡ and Joseph Kraut‡

Department of Chemistry, University of California, San Diego, La Jolla, California 92093, and Department of Biochemistry, Walter Life Science Building, University of Tennessee, Knoxville, Tennessee 37996

Received June 14, 1991; Revised Manuscript Received September 11, 1991

ABSTRACT: A remarkable correlation has been discovered between fluorescence lifetimes of bound NADPH and rates of hydride transfer among mutants of dihydrofolate reductase (DHFR) from *Escherichia coli*. Rates of hydride transfer from NADPH to dihydrofolate change by a factor of 1000 for the series of mutant enzymes. Since binding constants for the initial complex between coenzyme and DHFR change by only a factor of 10, the major portion of the change in hydride transfer must be attributed to losses in transition-state stabilization. The time course of fluorescence decay for NADPH bound to DHFR is biphasic. Lifetimes ranging from 0.3 to 0.5 ns are attributed to a solvent-exposed dihydronicotinamide conformation of bound coenzyme which is presumably not active in catalysis, while decay times (τ_2) in the range of 1.3 to 2.3 ns are assigned to a more tightly bound species of NADPH in which dihydronicotinamide is sequestered from solvent. It is this slower component that is of interest. Ternary complexes with three different inhibitors, methotrexate, 5-deazafolate, and trimethoprim, were investigated, along with the holoenzyme complex; 3-acetylNADPH was also investigated. Fluorescence polarization decay, excitation polarization spectra, the temperature variation of fluorescence lifetimes, fluorescence amplitudes, and wavelength of absorbance maxima were measured. We suggest that dynamic quenching or internal conversion promotes decay of the excited state in NADPH–DHFR. When rates of hydride transfer are plotted against the fluorescence lifetime (τ_2) of tightly bound NADPH, an unusual correlation is observed. The fluorescence lifetime becomes longer as the rate of catalysis decreases for most mutants studied. However, the fluorescence lifetime is unchanged for those mutations that principally alter the binding of dihydrofolate while leaving most dihydronicotinamide interactions relatively undisturbed. The data are interpreted in terms of possible dynamic motions of a flexible loop region in DHFR which closes over both substrate and coenzyme binding sites. These motions could lead to faster rates of fluorescence decay in holoenzyme complexes and, when correlated over time, may be involved in other motions which give rise to enhanced rates of catalysis in DHFR.

The seminal article by McCammon and co-workers (1977) on motion in proteins generated considerable debate about the role of dynamics in determining protein function. Since that time computer simulations of protein thermal fluctuations have steadily improved. Now, some even include the surrounding solvent matrix (Levitt & Sharon, 1988). However, a clear understanding of how dynamic motions in enzymes influence activity remains unavailable. The qualitative idea of "the fluctuating enzyme" had been formulated earlier (Careri, 1974) along with the hypothesis that rapid conformational fluctuations correlate in time with catalytic activity. A later proposal (Karplus & McCammon, 1983) discussed a specific role for protein flexibility in optimizing donor–acceptor distances for enhanced tunneling probabilities during electron transport processes. Recently, it was suggested (Kraut, 1988) that motion of enzyme templates may influence rates of enzymic reactions by altering reaction transmission coefficients or barrier recrossing frequencies. The coupling of protein modes to bond-making or bond-breaking steps may introduce directionality to enzyme reactions and reduce barriers significantly (Karplus & McCammon, 1983). Despite all the speculation, investigators have struggled to obtain experimental evidence that demonstrates the involvement of protein dynamic motions in catalysis.

The notion that protein side chains, entire segments, and even domains can fluctuate is no longer in question. The important challenge is to devise a mechanism for correlating protein dynamic movements with function, even though these events have widely disparate time scales. In this report, we describe our efforts to combine rapid spectroscopic measurements with site-directed mutagenesis and high-resolution X-ray diffraction results in order to verify experimentally that protein fluctuations do influence rates of catalysis in dihydrofolate reductase (DHFR). By correlating altered turnover rates of a series of mutant enzymes with their fluorescence properties, we hope to suggest the involvement of dynamics in DHFR[1] catalysis.

Several characteristics of *Escherichia coli* DHFR suggest it is a good system for our purposes. First, DHFR is a small monomeric enzyme of MW 18 000 consisting of a single po-

† This work was supported by NIH NRSA Postdoctoral Fellowship GM 12262 to M.F.F., NSF CHE-8715561 to D.M., NIH GM10928 to J.K., and NIH GM 35308 to E.E.H.

* Authors to whom correspondence should be addressed.
‡ University of California, San Diego.
§ University of Tennessee.

[1] Abbreviations: 3-acetylNADPH, 3-acetylpyridine adenine dinucleotide phosphate (reduced form); DHF, dihydrofolate; MES, 2-(*N*-morpholino)ethanesulfonic acid; THF, tetrahydrofolate; TMP, trimethoprim; TCPC, time-correlated single photon counting; DHFR, dihydrofolate reductase; wtDHFR, wild-type dihydrofolate reductase; hDHFR, human dihydrofolate reductase. The letter–number–letter notation for mutant DHFRs, e.g., F137S, is read as follows: the first letter represents the IUPAC–IUB established one-letter amino acid code of the native residue, the number identifies the position of the native residue, and the second letter represents the code for the amino acid introduced by mutagenesis.

0006-2960/91/0430-11567$02.50/0

lypeptide chain of 159 amino acids. Second, DHFR is one of the most studied enzymes with extensive information available on enzyme–substrate and enzyme–inhibitor interactions from X-ray crystallography (Matthews et al., 1977, 1985; Bolin et al., 1982; Bystroff et al., 1990), Raman (Osaki et al., 1981; Saperstein et al., 1978) and NMR spectroscopy (Birdsall et al., 1989; London et al., 1986; Cocco et al., 1983), numerous kinetic methods (Appleman et al., 1990; Morrison & Stone, 1988; Fierke et al., 1987), fluorescence and absorption measurements (Hood & Roberts, 1978; Poe et al., 1974), and molecular dynamic simulations (Dauber-Osguthorpe et al., 1988; Searle et al., 1988). Third, DHFR catalyzes the reduction of dihydrofolate (DHF) to tetrahydrofolate (THF) by NADPH. Enzymes involved in transferring hydrogen to and from nicotinamide cofactors represent over 15% of known enzymes. Since considerable information already exists on the rate and mode of hydride transfer in several specific enzyme reactions (Cha et al., 1989, and references therein), a demonstrated role of dynamics in activating NADPH for catalysis in DHFR would have wide-ranging mechanistic implications. Finally, *E. coli* DHFR has been cloned, overexpressed, and investigated using site-directed mutagenesis techniques (Benkovic et al., 1988; Villafranca et al., 1983). We could select mutations that minimally perturb the molecular structure, but have significant effects upon catalytic activity, and then ask whether there is any correlation between fluorescence properties and catalysis and, if so, whether there is any hint that dynamic motion plays a role.

An additional incentive for exploring the DHFR–NADPH system is the potential to monitor fluorescence of the cofactor and avoid extrinsic probes. Fluorescence is both selective and sensitive. Fluorescence behavior can be complex, but if it can be understood, it should be widely applicable. Excited states of enzyme-bound chromophores can decay not only by photon emission but also by a variety of nonradiative processes. It is quite common for the radiative probability per picosecond to remain constant, while competing nonradiative processes affect the state lifetime. Consequently, a measurement of the lifetime amounts to a measurement of the nonradiative process. One efficient decay mechanism for excited states of nitrogen-containing heterocycles possessing carbonyl functionalities such as NADPH is internal conversion through the proximity effect (Lim, 1986). In this process, systems having close-lying (proximate) $n\pi^*$ and $\pi\pi^*$ levels in the excited electronic state can rapidly dissipate energy through vibrational relaxation rather than photon emission. Results of Hones and co-workers (Fischer et al., 1988) on the influence of solvent effects upon the fluorescence properties of dihydronicotinamide model compounds suggest that interactions between solvent or protein environments with the carboxamide group of NADPH determine the relative stability of the excited state. Such interactions may promote internal conversion pathways as described above. Raman data confirm the importance of the carboxamide group in forming excited states of dihydronicotinamides (Bowman & Spiro, 1980). It is likely that the strong intermolecular contacts observed between backbone groups of enzymes and the carboxamide moiety of NADPH in X-ray structures of several NADP dehydrogenases influence the decay of the excited state of bound dihydronicotinamide. A variety of nonradiative mechanisms might be postulated; the more plausible alternatives are evaluated in the Discussion section.

Material and Methods

Substrate and inhibitors were purchased from Sigma with the exception of 5-deazafolate, which was provided by Dr. John Montgomery (Kettering Meyer Laboratory, Southern Research Institute, Birmingham, AL). Mutant DHFR proteins were prepared as previously described (Howell et al., 1986) using a line of host cells deficient in chromosomal wild-type DHFR and possessing resistance to kanamycin (Howell et al., 1988). Tightly bound nucleotides were removed in a final purification step employing methotrexate affinity chromatography.

In order to explore the dynamic flexibility of DHFR, we have determined fluorescence properties of NADPH free in solution and bound to mutant DHFR proteins, using time-correlated single photon counting (TCPC). TCPC was performed on a versatile picosecond fluorescence apparatus (Magde et al., 1990) consisting of a mode-locked argon ion laser (SpectraPhysics) set to synch-pump a tunable dye laser equipped for cavity dumping. Pulses of about 10-ps duration were available at any wavelength from about 550 nm to the near-IR region. Frequency doubling by harmonic generation provided excitation wavelengths between 275 and 400 nm at repetition rates of 2–4 MHz. An excitation wavelength of 328 nm was used in most experiments; 1024 channels were recorded, each representing a time window of 20–40 ps. The instrument response function was normally 70–100 ps. A 4-mL fused silica fluorescence cell was positioned within a thermostated sample chamber, and except for polarization studies, fluorescence was detected at the magic angle. Concentrations and buffers were the same as for steady-state fluorescence measurements described below. Integration times of 4–8 min were used, and the fluorescence counts peaked at a maximum of 4000–10 000 counts in the maximum channel. Fluorescence decays were deconvoluted to the best fit of a sum of exponentials given by

$$F(t) = \sum_{j=1}^{n} (\alpha_j e^{-t/\tau_j})$$

using a fast implementation of Marquardt nonlinear least squares. $F(t)$ is the measured fluorescence intensity at time t while α_j is the amplitude of the jth component having a lifetime τ_j.

Rates of hydride transfer and of ligand binding were measured on either a Durrum D110 or a HI-TECH SF-51 stopped-flow instrument with empirical dead times of 2.8 and 1.8 ms, respectively. The pre-steady-state burst of product formation was monitored by following the decrease in fluorescence energy transfer to bound NADPH during initial enzyme turnovers (Fierke et al., 1987). Fluorescence was detected at 450 nm through a narrow band (10-nm) interference filter (Ealing Optics) using 290-nm excitation. Voltage transients were collected on a Datel 286 AT computer equipped with a MetraByte Dash16 A-to-D converter. Individual data points collected at the fastest rate (50 KHz) were computer averaged when sampling periods longer than 20 μs were used. Fluorescence rates from at least four individual shots were averaged and then fit to a single-exponential burst or a single-exponential burst followed by a linear rate using the program NONLIN, a PC implementation of Marquardt nonlinear least squares written in Turbo Basic. A typical shot involved rapid mixing a solution of premixed enzyme–cofactor complex with a solution of dihydrofolate. Final concentrations of reactants were typically 15 μM dihydrofolate reductase, 125 μM NADPH, and 120 μM DHF in buffer containing 50 mM Tris, 25 mM MES, 25 mM acetic acid, and 0.1 M KCl at pH 5.5 or 44 mM imidazole, 44 mM diethanolamine, 33 mM succinic acid, and 0.1 M NaCl. Dihydrofolate concentrations as high as 300 μM were also tested to eliminate any depen-

dence of k_{obs} on the rate of ligand binding. Enzyme and cofactor were premixed in dilute Tris buffer at pH 8.0 for at least 5 min to remove hysteretic behavior and then added to concentrated buffer at pH 5.5. This strategy minimized acid-catalyzed degradation of NADPH prior to rapid mixing. NADPD was prepared as previously described (Morrison & Stone, 1988).

Steady-state fluorescence measurements were made on an SLM-Aminco Model SPF-500 spectrofluorometer operating in ratio mode. Fluorescence spectra were collected in a 4.0-mL fluorescence cell (thermostated) containing samples of mutant DHFR proteins (15 μM) in 10 mM Tris-HCl, pH 8.0, with 0.1 M NaCl and 14 μM NADPH where appropriate. Inhibitor complexes were formed by adding a slight excess of inhibitor to premixed holoenzyme samples. Excitation spectra were collected by monitoring fluorescence emission at 450 nm (2.5- or 5.0-nm slit) while scanning excitation wavelengths from 230 to 400 nm. Polarization excitation spectra were obtained in a similar manner by collecting fluorescence spectra using two film polarizers, one for excitation and the other for emission, set in all four possible combinations of orientations, horizontal or vertical for each. Final polarization spectra were corrected by computer calculation for differences in instrument detection efficiency at different wavelengths. Emission spectra were generated by following fluorescence emission from 350 to 500 nm after 280- or 290-nm excitation.

Absorption difference spectra were obtained on a Perker Elmer λ 3B UV/vis spectrophotometer using a split-cell cuvette in a temperature-regulated cell holder. Samples contained 15 μM DHFR and 14 μM NADPH in 10 mM Tris-HCl buffer at pH 8.0 and 0.1 M NaCl. Absorbance traces from 250 to 400 nm were recorded on a Datel 286 computer running the program UVS (Softways, Inc.). Difference spectra were obtained by computer subtraction of scans before and after mixing the contents of the split cell, each side having a 0.45-cm path length.

Results

Binding and Catalysis in Mutants of DHFR. Rate constants for association and dissociation reactions of NADPH to apoDHFRs were determined using the relaxation method in the stopped-flow apparatus (Fierke et al., 1987). Rates of nicotinamide dissociation from holoenzyme complexes were also determined in competition experiments. As indicated in Table I, binding affinities were largely unaffected by mutations in wtDHFR. Two mutations within the cofactor nicotinamide binding site, T46V and T46A, produced enzymes with elevated off rates for reduced coenzyme such that their dissociation constants for NADPH increased 10–15 times. Even in these instances, perturbations were modest, suggesting that the nicotinamide group does not significantly contribute to observed tight binding of reduced NADP to holoDHFR.

We evaluated catalytic potential in mutant enzymes by measuring catalysis separately from substrate binding and product dissociation. The catalytic reaction of DHFR, in which a hydride ion is transferred directly from NADPH to the C6 of dihydrofolate, was monitored directly by stopped-flow methods. Measured rate constants for the pre-steady-state burst of product formation ranged from about 1000 s^{-1} for F137S DHFR to 1.0 s^{-1} for D27C DHFR. Deuterium isotope effects on the burst at pH 5.2 ranged from 2.3 for F137S to 4.0 for S49V. Although the measured isotope effects for F137S and wtDHFRs are somewhat less than 3.0 (the value measured in the steady state at pH 9.0), they suggest that hydride transfer is nearly rate-limiting in pre-steady-state reactions (Northrup, 1977). All reactions were run at pH 5.5 or below where ternary complexes of enzyme–NADPH–DHF are fully protonated for most mutants (Fierke et al., 1987). When steady kinetic pH profiles (J. Hirai, M. Warren, and C. David, personal communication) revealed an altered pK_a for catalysis by mutant enzymes, hydride transfer rates were determined at several pH values over the range of 5–8. Therefore, best estimates of pH-independent rates for hydride transfer are given in Table I. Effects of glycerol and temperature upon catalysis in wtDHFR were also measured.

Table I: Kinetic Binding Constants for Enzyme Cofactor Complexes and Rates of Hydride Transfer for Mutants of Dihydrofolate Reductase[a]

mutants	k_{on} (μM^{-1} s^{-1})	k_{off} (s^{-1})	k_{off}/k_{on} (μM)	k_{hyd} (s^{-1})
F137S	15 ± 2.0[b]	6 ± 3[b]	0.40 ± 0.20	930 ± 115
WT	18 ± 1.0[b]	10 ± 4[b]	0.56 ± 0.22	678 ± 83
D27E	15 ± 1.2	22 ± 1	1.5 ± 0.12	430 ± 53
D27S, F137S	18 ± 1.0[b]	30 ± 5[b]	1.7 ± 0.30	288 ± 23
R44T	ND	ND	ND	280 ± 30
D27S	11 ± 3.0[b]	38 ± 6[b]	3.4 ± 1.1	267 ± 5
W22F	15 ± 2.9	8 ± 2[d]	0.53 ± 0.17	263 ± 43
S49V	12 ± 3.1	19 ± 2	1.6 ± 0.43	210 ± 23
T46A	8.4 ± 0.5	77 ± 6[d]	8.4 ± 2.8	112 ± 16
D27N	9.6 ± 1.3[c]	14 ± 8[c]	1.4 ± 0.82	91 ± 17
T46V	9.2 ± 3.0	126 ± 6[d]	15 ± 1.1	78 ± 12
D27E + AH[e]	ND	ND	ND	11 ± 2
W2	14 ± 1.0	28 ± 1	2.0 ± 0.16	5.8 ± 1.3
D27	13 ± 1.5	30 ± 3	2.3 ± 0.35	1.0 ± 0.2

[a] Hydride transfer rates were measured at 20 °C as described under Materials and Methods. Ligand association and dissociation rates were measured (20 °C) in the stopped-flow experiments using solutions buffered with 10 mM Tris-HCl at pH 8.0 containing 0.1 M KCl. [b] From Dunn et al. (1990). [c] From Appleman et al. (1990). [d] Determined by competition methods (Fierke et al., 1987). [e] 3-acetyl-NADPH.

A more complex procedure was necessary to estimate hydride transfer rates for the fully competent enzymes having mutations at position 27. These enzymes require preprotonated dihydrofolate for activity. To obtain pH-independent values for hydride transfer, the steady-state pH profiles for k_{cat} and k_{cat}/K_m were refitted to the equations given previously (Howell et al., 1987), using the recently redetermined pK_a of 2.6 for the N5 of DHF (Maharaj et al., 1990). Most calculated values for hydride transfer are now higher than previously reported.

Fluorescence Decay of Reduced Coenzyme in Solution. Fluorescence decay curves of NADPH in solution are fit best by a double-exponential equation. Decay is rapid and biphasic, confirming earlier results of Visser and van Hoek (1981). The relative proportions of the two phases and lifetimes shift with changing temperature. Decay lifetimes (τ) ranging from 0.1 to 0.3 ns for a fast component and from 0.4 to 0.7 ns for a slower phase were assigned to fluorescence decay from open and closed forms of NADPH in solution, respectively (Visser & van Hoek, 1981). Much more rapid emissive decay was observed for the excited state of 3-acetylNADPH where a single lifetime of 0.22 ns was adequate.

Fluorescence Decay of NADPH in Mutant Holoenzyme Complexes. Fluorescence lifetimes of NADPH increase as much as 300% when the coenzyme is bound to DHFR (τ_2 in Table II). Similar increases in observed lifetime of NADPH to 1.5 and 2.0 ns have been reported for holoenzyme complexes of malate and lactate dehydrogenases, respectively (Baumgarten & Hones, 1988). As illustrated in Figure 1, fluorescence decay of NADPH bound to DHFR remains double exponential. The fractional amplitude of the longer decay process reached a maximum value of 60% in the S49V mutant binary complex and a low value of 28% when bound to T46V

Table II: Fluorescence Lifetimes (τ, in nanoseconds) and Fractional Amplitudes (f) of NADPH Bound to DHFR Mutants[a]

	holoenzymes				TMP complexes	
DHFR mutants	f_1	τ_1	f_2	τ_2	f_2	τ_2
D27N	60.0	0.31	40.0	1.27	60.0	2.91
D27C	57.3	0.39	42.7	1.34	81.0	2.50
D27S	47.0	0.56	53.0	1.39	86.0	3.00
D27S, F137S	41.0	0.30	59.0	1.41	60.0	2.67
WT	43.8	0.30	56.2	1.43	65.0	2.10
R44T	70.0	0.35	30.0	1.44	85.6	2.17
S49V	40.0	0.31	60.0	1.44	85.6	2.28
F137S	59.0	0.36	41.0	1.52	86.7	2.31
D27E	42.0	0.39	58.0	1.58	86.7	2.53
W22F	56.0	0.33	44.0	1.83	36.0	3.43
T46A	72.6	0.57	27.8	1.83	86.0	1.91
T46V	68.0	0.52	32.0	1.93	68.0	2.02
W22H	50.0	0.43	50.0	2.20	41.4	3.08
WT + AH[b]	68.0	0.26	32.0	2.28	100	2.80
hDHFR	46.6	0.43	53.4	1.93	40.0	1.57

[a] Fluorescence decays (328-nm excitation; 450-nm emission) were collected as described under Materials and Methods. Enzyme concentrations were 15 μM while coenzyme levels were kept slightly lower at 14 μM in a total volume of 3.5 mL of 10 mM Tris buffer at pH 8.0. A slight excess of TMP (16 μM) was added to form ternary complexes. [b] 3-acetylNADPH.

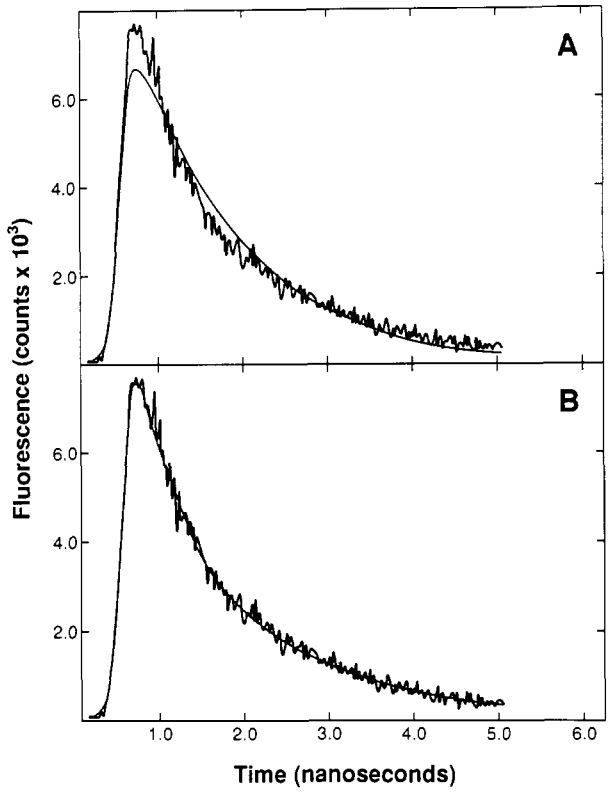

FIGURE 1: Time dependence of fluorescence decay of NADPH bound to T46A DHFR. A double-exponential fit, shown in panel B, is compared to single-exponential modeling illustrated in panel A. Measurements were performed as described in the text. Not shown is a reference pulse measured simultaneous with the sample fluorescence signal that provided an internal check against spurious shifts in the time base.

DHFR (cf. Table II). The slower component made up only 32% of the decay process for 3-acetylNADPH bound to wild-type DHFR. Decay times (τ_2) varied from 1.27 ns for NADPH bound to D27N to 2.20 ns for coenzyme complexed to W22H DHFR. Close inspection of fluorescence decay curves for holoenzymes of D27C and D27N mutants reveals that a continuous distribution of exponentials rather than two distinct decay times more accurately describes emissive decay

Table III: Temperature Variation of Lifetimes (in nanoseconds) of Long Relaxation (τ_2) for NADPH in Holoenzymes and Ternary Complexes of Trimethoprim with Mutant DHFR Proteins[a]

		lifetime[b] (ns)					
mutant	complex	10.6 °C	15.3 °C	20.0 °C	25.0 °C	29.8 °C	
D27N	NH	1.37	1.31	1.24	1.22	1.17	
	TMP	ND	3.32	(2.99)	ND	2.73	
D27C	NH	1.49	1.39	1.37	1.23	1.24	
	TMP	2.83	2.57	2.50	2.39	2.09	
D27S	NH	1.55	1.49	1.42	1.36	1.21	
	TMP	3.32	3.16	(2.85)	2.56	2.34	
D27S, F137S	NH	1.56	1.52	1.41	1.36	1.29	
	TMP	ND	3.16	(2.75)	2.67	ND	
WT	NH	1.62	1.54	1.43	1.34	1.24	
	TMP	ND	2.24	1.95	ND	1.84	
R44T	NH	1.60	1.50	1.38	1.27	1.18	
	TMP	2.23	2.05	1.97	1.76	1.59	
S49V	NH	1.62	1.55	1.47	ND	1.42	
	TMP	2.60	2.41	2.28	1.94	1.91	
F137S	NH	1.79	1.65	1.52	ND	1.34	
	TMP	2.74	2.58	2.47	2.30	2.26	
D27E	NH	1.78	1.68	1.58	1.47	1.37	
	TMP	2.97	2.79	2.51	2.19	1.98	
W22F	NH	2.04	1.97	1.85	1.78	1.65	
	TMP	3.83	3.51	3.34	3.04	2.76	
T46A	NH	2.10	2.06	1.83	1.68	1.66	
	TMP	2.62	2.19	2.03	1.74	1.58	
T46V	T46A	NH	2.33	2.0	2.07	1.93	1.87
	TMP	2.43	2.21	1.91	1.69	1.40	
W22H	NH	2.57	2.45	2.29	2.16	2.00	
	TMP	3.40	3.05	2.80	2.46	2.22	
hDHFR	NH	2.02	1.98	1.96	1.89	1.83	
	TMP	ND	ND	(1.57)	ND	ND	

[a] Conditions were as described in Table II. Inhibitors were added to preformed holoenzyme complexes to give final inhibitor concentrations of 16 μM. [b] Values in parentheses were measured at 22 °C.

in these complexes. In all cases, changes in lifetime were accompanied by corresponding changes in fluorescence quantum yield. Radiative rate constants are unchanged; only nonradiative decay processes are changing.

Temperature Dependence of Fluorescence Decay Parameters for Parent and Mutant DHFR Complexes. Decay curves for all mutant holoenzymes and ternary enzyme–trimethoprim–NADPH complexes were collected at several temperatures from 11 to 30 °C. As shown in Table III, lifetimes of the longer emissive phase change with temperature for both types of complexes. Decay rates became slower (longer τ values) at lower temperatures, producing an increase in overall fluorescence yield for all samples. Changes in lifetimes were more dramatic for some enzyme complexes than others.

Time-Dependent Polarization of Fluorescence from Mutant DHFR Complexes. Polarization effects upon fluorescence amplitudes, fluorescence lifetimes, and overall fluorescence intensities for several enzyme complexes were measured on the TCPC apparatus. Fluorescence is positively polarized, and the anisotropy decays at a rate that approximately matches the rotational correlation time of DHFR. Since the fluorescence decays much faster than the rotation, it was not possible to measure accurately the rotational correlation time. It is clear, however, that the majority of the fluorescence comes from a tightly bound species that remains rigidly fixed to the protein. This general behavior was observed in all cases examined. In addition, there was evidence for a rapidly decaying component of the emission polarization at very short times (<0.5 ns). Such a component might be attributed to a more mobile conformation for the rapidly decaying component seen in the total (magic-angle) fluorescence decay, but it could also include the effect of small amplitude, short-time "wobbling" of the protein-bound form.

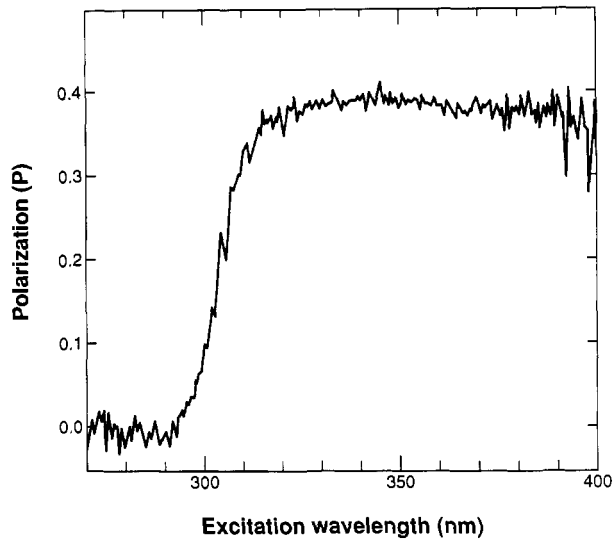

FIGURE 2: Steady-state fluorescence excitation polarization spectrum for the holoenzyme complex of wild-type DHFR. Spectra were recorded as described under Materials and Methods. The final polarization spectrum has been corrected for differences in instrument response at various wavelengths.

We performed one exploratory measurement on a ternary complex. The complex of wtDHFR with TMP showed virtually no change in polarization from that observed for the corresponding holoenzyme. This suggests that there is no energy transfer prior to emission in that complex.

Excitation Polarization Spectra. In order to detect possible fluorescence emission from excited states that differ from the state or transition involved in photon absorption, steady-state polarization excitation spectra were measured for complexes of several DHFR mutants. As shown in Figure 2, polarization values of fluorescence emission for bound NADPH remain relatively constant at a value near 0.40 for excitation wavelengths above 320 nm. Below 290 nm, polarization values near zero suggest emission occurs from a relaxed excited state that has its emission dipole oriented, on the average, close to 55° relative to the moment giving rise to absorption. An emission peak at 285 nm in the corrected excitation spectrum is likely due to resonance energy transfer from the excited state of protein tryptophan residues to the dihydronicotinamide ring.

The excitation polarization spectrum for the holoenzyme of wtDHFR in 45% glycerol was nearly the same as the spectrum observed in normal aqueous solvents. In fact, the polarization value of 0.41 remains essentially constant over the range of excitation wavelengths from 310 to 410 nm. Glycerol also had a minimal effect on the emission spectrum of wtDHFR, despite an increased value of the fluorescence lifetime of bound NADPH. The conclusion that one absorbing and one emitting state dominate is further supported by a wavelength-independent value of 0.39 for the observed polarization across the entire emission spectrum of NADPH bound to wild-type DHFR following excitation at 330 nm.

Complexes of mutant enzymes with three different inhibitors exhibited several interesting differences in excitation polarization spectra when compared to those of holoenzymes. Trimethoprim complexes had identical limiting polarization values at high wavelengths, i.e., 0.39, and a similar overall shape for the polarization curve. Spectra for ternary complexes with another inhibitor, methotrexate, were different. For the wtDHFR complex, the limiting polarization was 0.19 compared to 0.39 for the holoenzyme. This is significant because in time-resolved decay experiments on the methotrexate ternary complex the long relaxation process attributed to bound dihydronicotinamide is severely quenched. Both the lifetimes and the yield plummet. In this complex, low-intensity fluorescence emissions originate from a species of NADPH behaving like solution coenzyme. The lifetime of the fast phase (τ_1) for the wtDHFR–NADPH–methotrexate complex is similar to the average decay time for NADPH in solution. Identical excitation polarization spectra for the wild-type methotrexate ternary complex and solution NADPH confirm that similar species emit photons for both molecules. We assign the rapid phase in fluorescence decay curves of holoenzyme complexes and ternary complexes with methotrexate to a more solvent-exposed form of bound NADPH. Fully complexed dihydronicotinamide presumably undergoes an efficient excited state interaction with methotrexate that leads to enhanced nonradiative decay. A third inhibitor, 5-deazafolate, exhibited still different properties. Some fluorescence is observed at long lifetimes because 5-deazafolate itself fluoresces at 450 nm. A shifted intensity maximum in the emission spectrum and a reduced limiting polarization value, 0.25, in the excitation polarization spectrum confirm energy transfer or exciplex formation between NADPH and inhibitor. The longer lived emission component is attributed to a species that is predominately 5-deazafolate in character.

Time-Resolved and Steady-State Fluorescence Spectra. The fluorescence spectra of the holoenzyme and ternary complex with TMP were examined for possible changes over time. Time slices of 0–200 ps, 0.500–1.0 ns, and 1.5–2.0 ns were selected by a method described previously (Rojas & Magde, 1983). A 5-nm band-pass was used. At early times, 0–200 ps, a slight but noticeable excess in fluorescence intensity is observed at longer wavelengths (>475 nm) compared to spectra taken at longer time slices of 0.5–1.0 ns and 1.5–2.0 ns. This difference presumably reflects slight energy differences between ground and excited states for a fast-decaying, less tightly bound dihydronicotinamide species. Time-resolved spectra for ternary complexes of trimethoprim had intensity maxima shifted to higher energy (425 nm) compared to the corresponding holoenzyme complex. However, no time-dependent differences in intensities were detected at longer wavelengths.

Steady-state fluorescence spectra were collected for several samples to confirm that fluorescence emission occurs from excited states with similar energies in all holoenzyme complexes. Differences in emitted fluorescence intensity were readily apparent, indicating different fluorescence yields. Normalized spectra, however, looked essentially identical for all DHFRs, including wtDHFR in glycerol. Lower temperatures (17 °C) also did not produce significant spectral shifts in fluorescence spectra. Excitation spectra were collected for several mutant holoenzymes between 230 and 400 nm. Because samples contained equal amounts of complexed coenzyme, fluorescence intensity differences following excitation at 340 nm indicate that mutant DHFR proteins have different quantum yields. These results agree with the total integrated fluorescence intensity under time-resolved decay curves for each holoenzyme. Finally, relative intensities of fluorescence detected at 450 nm were measured following excitation between 260 to 290 nm and 320 to 370 nm. Fluorescence excited by 290-nm excitation results from energy transfer between tryptophans and NADPH while emission following 340-nm excitation represents direct nicotinamide excitation. Ratios of fluorescence intensities at 290 and 340 nm, respectively, therefore provide a rough measure of efficiency for resonance energy transfer between protein tryptophans and bound coenzyme in each complex. This ratio varies from 0.79 for

D27C, D27E, and wtDHFR to 0.52 for W22F DHFR. Removal of Trp22 in W22F DHFR reduces the overall amount of energy transfer. The absence of significant differences in energy transfer for enzymes containing all their native tryptophans suggests that the changes in hydride transfer and fluorescence decay rate are due to critical local effects and not to any major changes in overall geometry of the protein.

Absorption Difference Spectra. Absorption difference spectra for liganded NADPH showed variable wavelength maxima among mutant holoenzyme complexes that correlate to some extent with enzyme activity. The wavelength for maximum difference in absorbance shifts from 350 nm in wtDHFR–NADPH to 356 nm in W22H–NADPH at 23 °C. W22H DHFR catalyzes hydride transfer at roughly 1% of the activity of wild-type DHFR. Intensity differences for absorbance changes near 350 nm appear to match relative proportions of dihydronicotinamide bound tightly to DHFR as detected in relative amplitudes of the long decay process in time-resolved decays of fluorescence. For W22H DHFR, the change in absorption between bound and unbound cofactor is only 60% of the change for wild-type DHFR (0.0090/0.017 absorbance units). Similarly, the relative amplitude of the long decay process during fluorescence decay is only 50% for W22H DHFR while it is close to 65% for the wild-type enzyme.

Absorption difference spectra for several enzyme complexes were also measured at various temperatures. The maximum change in absorbance for wild-type and mutant DHFRs shifted to longer wavelengths (lower energy) in response to elevated temperatures. A greater shift occurred for the wild-type holoenzyme when the temperature rose from 15 to 23 °C (2 nm) than from 23 to 30 °C (1 nm). Corresponding changes in absorption for NADPH bound to W22F DHFR were less significant. For holoenzyme complexes of wild-type DHFR in 35% glycerol, the maximum in the difference spectrum occurred at shorter wavelengths (344 nm at 15 °C) and shifted similarly to longer wavelengths at elevated temperature when compared to pure aqueous samples of wtDHFR.

Relationship between Catalysis and Fluorescence Decay of NADPH in Holoenzyme of Mutant DHFRs. Surprisingly, fluorescence lifetimes (τ_2) for NADPH in holoenzyme complexes correlate with measured rates of enzyme-catalyzed hydride transfer for most mutant DHFRs. As illustrated in Figure 3, DHFRs with faster rates of fluorescence decay of reduced coenzyme also catalyze hydride transfer most effectively. In our preliminary report of this phenomena, we proposed that a near-linear correlation for most mutants implied that a direct relationship exists between the mechanisms leading to rapid decay of the excited state and to enhanced rates of catalysis (Farnum et al., 1990). D27C and D27S DHFRs represented unexplained deviations from a linear relationship. Fluorescence decay and catalysis parameters for the D27S, F137S double, and D27N single mutant proteins gathered more recently in this investigation establish another limb of the curve for rapid decays where no correlation exists between catalysis and emissive decay. Our model, therefore, attempts to explain not only the apparent correlation between fluorescence and catalytic properties of DHFRs on the major limb at moderate to long decay times but also its clear breakdown at short decay times.

Summary of Important Results. For convenient reference, we summarize those results most central to the following discussion.

(1) Fluorescence decay of NADPH in solution is rapid and biphasic. The lifetimes of the fast and slow components range from 0.1 to 0.3 ns and 0.4 to 0.6 ns, respectively. The fast phase is attributed to the open form of NADPH while the slower component corresponds to fluorescence decay from the stacked conformation (Visser & van Hoek, 1981).

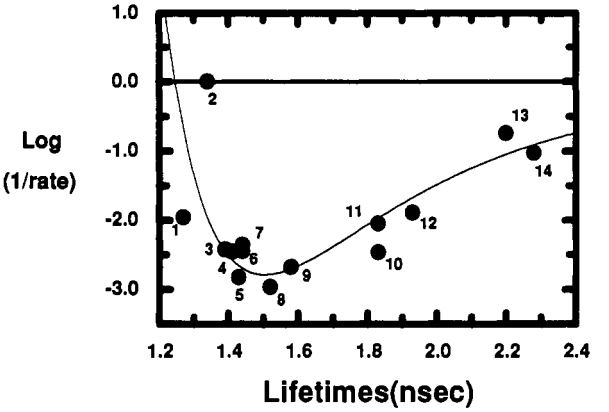

FIGURE 3: Fluorescence lifetime (τ_2) of NADPH in mutant DHFR binary complexes plotted against the logarithm of catalytic flux ($1/k_{hydride}$). The following equation was used to draw a smooth curve through the data points: $\log (1/k_{hydride}) = A(1/\tau_2 + \tau_{soln}))^{11} - B((1/\tau_2 + \tau_{soln}))^6$, where $\tau_{soln} = 0.8$, $A = 2.5 \times 10^4$, and $B = 8 \times 10^2$. Error estimates for hydride transfer vary from a maximum of 15% for F137S DHFR to a low of 5% for D27C DHFR. A maximum uncertainty of 0.1 ns applies to the fluorescence decay time. Numbering scheme: 1, D27N; 2, D27C; 3, D27S; 4, D27S,F137S; 5, wtDHFR; 6, R44T; 7, S49V; 8, F137S; 9, D27E; 10, W22F; 11, T46A; 12, T46V; 13, W22H; 14, 3-acetylNADPH.

(2) When NADPH is bound to mutants of *E. coli* DHFR, two fluorescent phases are again detected. A fast component with a largely invariant lifetime of 0.4 ns represents nearly 50% of the initial amplitude (but only 10% of the total yield) while a longer lived species has lifetimes in the range of 1.3–2.2 ns. The latter lifetimes vary among different mutant holoenzymes. As detailed below, we assign the fast component to a more solvent-exposed, solution-like conformation of bound coenzyme and the long lived species to NADPH with the dihydronicotinamide ring tightly bound and sequestered from bulk solvent.

(3) Lifetimes and intensities for both phases in the time course of fluorescence decay decrease with increasing temperature.

(4) The fluorescence lifetime of the bound 3-acetyl- analogue of NADPH is more than 50% longer than bound NADPH, despite the fact that the analogue decays twice as fast in solution.

(5) Fluorescence lifetimes of all complexes increase markedly when trimethoprim occupies the pterin binding site; they increase further at lower temperatures. In contrast, methotrexate efficiently quenches fluorescence of bound NADPH.

(6) The holoenzyme complex of human DHFR has a longer fluorescence lifetime, 1.9 ns, than that of wild-type *E. coli* enzyme. However, the binding of trimethoprim produced opposite effects in ternary complexes. The lifetimes changed from 1.9 to 1.5 ns in human DHFR and from 1.4 to 2.1 ns in *E. coli* DHFR. Note that TMP binds with different geometry to vertebrate and *E. coli* DHFRs (Champness et al., 1986; Matthews et al., 1985).

(7) Excitation polarization spectra of binary complexes look identical among the mutant enzymes with samples having a limiting value near 0.40 at exciting wavelengths between 320 and 400 nm. Trimethoprim had no effect on the limiting polarization value; methotrexate, however, produces a spectrum similar to that of solution NADPH. Because of the low value of 0.17 for the limiting polarization of NADPH in solution and in the ternary methotrexate complex, the absorption and

emission dipoles of coenzyme must be almost orthogonal compared to their orientations when NADPH is bound tightly to holoDHFR. These results suggest that most of the fluorescence from bound dihydronicotinamide is quenched upon methotrexate binding while emission from the more solvent exposed conformation remains unaffected.

(8) Time-resolved fluorescence spectra of several mutant–coenzyme binary complexes were quite similar for time slices of 0–200 ps, 1.0–1.5 ps, and 1.5–2.0 ps after nicotinamide excitation except that slightly more fluorescence intensity was observed at wavelengths longer than 470 nm in early, 0–200 ps, compared to late, 1.5–2.0 ps, time windows for all measured samples.

(9) Steady state fluorescence emission spectra from 350 to 500 nm were not significantly different among the mutant enzymes. However, binding of trimethoprim shifts the wavelength of maximum fluorescence intensity from 450 nm in holoDHFRs to 425 nm in the ternary complex.

(10) The wavelength of the maximum absorbance difference that occurs upon binding NADPH to DHFRs shifts from 350 nm in wtDHFR to 356 nm in W22H DHFR at 23 °C. Maxima shift to longer wavelengths as the temperature is raised. For wtDHFR, the change in absorbance maximum with temperature is more pronounced. Little change occurred for W22F DHFR over the temperature range of 17–30 °C. In addition, glycerol shifted the wtDHFR maxima from 350 to 344 nm.

(11) A correlation exists between the rates of fluorescence decay for bound NADPH and rates of hydride transfer among most mutants. Most mutants show slower hydride transfer and longer decay times. Other mutant enzymes, particularly those with mutations at position 27, have fluorescence decay rates as fast as or faster than that of wtDHFR. For these proteins, no relationship is observed between catalysis and fluorescence decay rates.

Discussion

Mechanisms of fluorescence decay are often complex. Nevertheless, the data presented above suggest that some pathways are more likely than other to contribute to decay of the excited state in NADPH–DHFR. After reviewing spectroscopic data on dihydronicotinamide compounds, we will first argue that static quenching and solvent relaxation, two common decay pathways in protein–chromophore complexes, are unlikely mechanisms for excited state deactivation in DHFR. Next, we will marshal evidence in favor of dynamic quenching by enhanced internal conversion as the dominant process determining fluorescence lifetimes. Then, using recently determined X-ray diffraction structures, we will examine several interactions of DHFR with the dihydronicotinamide ring of NADPH as possible origins of the correlation between fluorescence decay and catalysis for the series of mutant enzymes.

Electronic Transitions of Enzyme-Bound Dihydronicotinamides. The relatively intense 340-nm absorption band (ϵ = 6200 M^{-1} cm^{-1}) of NADPH is considered to be a π–π^* transition involving the dihydronicotinamide ring and carboxamide group. Experimental estimates of dipole moments of 1-methyl-1,4-dihydronicotinamide suggest that the excited state of NADPH is more polar than the ground state (Evleth, 1967). This conclusion is supported by observations of significant blue shifts (higher energies) of π–π^* transitions of dihydronicotinamides in nonpolar solvents (Fischer et al., 1988). MO calculations indicate that formation of the excited state causes considerable charge density to develop in the

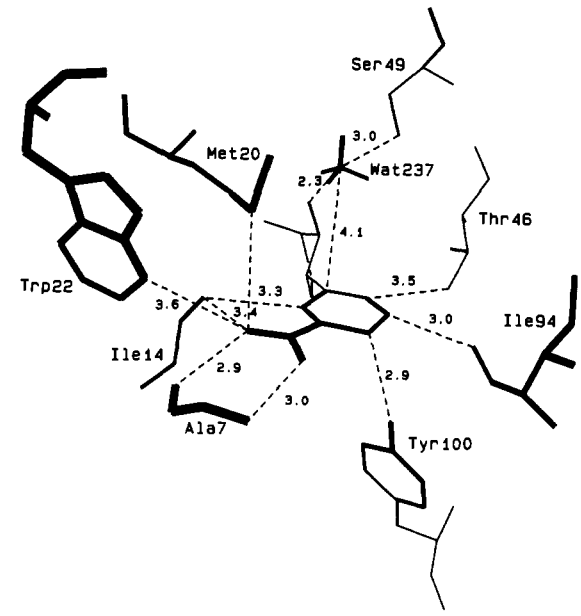

FIGURE 4: Structure of NADPH binding site in ternary folate–$NADP^+$ complex of *E. coli* DHFR showing key interactions of enzyme with the nicotinamide ring of $NADP^+$. The van der Waals surfaces of Met20 and the carboxamide group attached to the dihydropyridine ring of the coenzyme reveal the close contact between the Met20 sulfur atom and the amide nitrogen of NADPH. Contacts close enough to form reasonable hydrogen bonds are highlighted.

carboxamide group attached to the dihydronicotinamide ring (Maggiora et al., 1969). Further, Raman and resonance Raman results confirm conjugation of the carboxamide with the dihydropyridine ring because a C=O stretch (frequency near 1680–1690 cm^{-1}) dominates both spectra (Bowman & Spiro, 1980; Deng et al., 1989b).

Recent results of Hones and co-workers (Fischer et al., 1988; Baumgarten & Hones, 1988) indicate hydrogen bonding interactions between solvent or protein surfaces and the carboxamide moiety influence absorption and fluorescence characteristics of dihydronicotinamides. Enhanced fluorescence quantum yields and increased molar absorptivies were observed in solvents capable of donating a proton to the carbonyl group. In contrast, solvents offering lone-pair acceptor sites for hydrogen bonding to the amide NH produced slight reductions in intensities and blue shifts of absorption extinction maxima. Because fluorescence spectra generally did not show a similar specific hydrogen bonding effect, increased charge at the amide nitrogen in the excited state was proposed to weaken this interaction.

X-ray diffraction results detail enzyme–coenzyme interactions in DHFR (Filman et al., 1982). As illustrated in Figure 4, backbone carbonyl groups of isoleucine side chains at positions 14 and 94, and side-chain hydroxyl groups of Tyr100 and Thr46 surround the nicotinamide ring in the cofactor binding site. These oxygen atoms appear to promote electron deficiency at C4 of dihydronicotinamide in the transition state by stabilizing partial positive charge development at positions C2, C5, and C6 of the dihydropyridine ring (Filman et al., 1982). The backbone amide and carbonyl groups of Ala7 act as hydrogen bond donor and acceptor, respectively, to the coenzyme carboxamide. Also, the backbone carbonyl oxygen of Ile-14 interacts with both the amide group of the nicotinamide and C2 of the dihydropyridine ring. These interactions help maintain planarity of the carboxamide group with the dihydropyridine ring. A conserved ordered water molecule interacts with N1 of the dihydropyridine ring of NADPH and with hydroxyl groups of Ser49 and nicotinamide ribose. This

water presumably serves to pyramidalize N1 of NADPH in the transition state of the hydride transfer reaction. Changes in any of these key protein–coenzyme interactions could alter fluorescence lifetimes of bound NADPH. Because the carboxamide group has a demonstrated role in determining fluorescence characteristics of dihydronicotinamides, however, our attention will primarily focus upon interactions of DHFR with the carboxamide of bound NADPH.

Different extinctions for NADPH when bound to different mutants of DHFR suggest variable hydrogen bond strengths between DHFRs and the carboxamide group. For instance, a maximum absorbance difference (Δabs) between NADPH free in solution and bound to W22H DHFR occurs red-shifted (356 nm) relative to the value observed for wild-type DHFR (351 nm). This indicates weakened hydrogen bonds between the amide group of NADPH and W22H DHFR (Baumgarten & Hones, 1988). The red shift in absorbance maximum for W22H DHFR parallels the longer wavelength absorbance maximum, 360 nm, for 3-acetylNADPH. This analogue cannot form a pair of hydrogen bonds with the Ala7 backbone because the carboxamide has been replaced with an acetyl.

Circular dichroism (CD) measurements of NADPH in solution and bound to several species of DHFR indicate the environment surrounding the coenzyme in *E. coli* DHFR is unique among DHFRs. A negative Cotton effect at 340 nm assigned to dihydronicotinamide was reported for spectra of complexes of NADPH with *Lactobacillus casei* (Hood et al., 1979), *Streptococcus faecium* (Freisheim & D'souza, 1971), and chicken liver DHFRs (Seng & Bolard, 1983). No changes were reported in this region for the *E. coli* DHFR–NADPH complex (Greenfield, 1975). The fact that no change occurs in rotational strength of the nicotinamide absorption upon binding to the *E. coli* enzyme may indicate either reduced electronic asymmetry of bound coenzyme or reduced overlap of electronic states compared to other holoDHFRs (Hood et al., 1979). A survey of amino acid sequences reveals a significant difference in composition at position 20. In *E. coli* DHFR, a methionine residue at position 20 interacts directly with the carboxamide of NADPH. In vertebrate and those bacterial DHFRs which show a negative Cotton effect in CD spectra of bound coenzyme, this residue is a leucine. Although CD spectra for ternary complexes of NADPH and methotrexate with all species of DHFR show similar evidence for an excited state interaction between methotrexate and NADPH, trimethoprim induces different changes in the CD spectra of holoDHFRs. When trimethoprim binds, a slight negative Cotton effect appears at 335 nm in *E. coli* DHFR while the negative band seen at 340 nm in the binary complex of *L. casei* (and presumably other DHFRs) disappears. Crystallographic results showing different positions of the trimethoxybenzyl group of TMP in ternary complexes of *E. coli* and chicken liver DHFRs (Champness et al., 1986; Matthews et al., 1985) may explain why trimethoprim induces different spectroscopic behavior in complexes with different DHFRs.

Eliminating Static Quenching and Dipolar Relaxation Mechanisms of Fluorescence Decay. The variation in fluorescence decay times with temperature observed in DHFR suggests that simple static quenching is not responsible for changes in fluorescence lifetimes of mutant complexes. Both fluorescence intensity and relaxation time decrease in holoenzymes as the temperature increases. This contrasts with the simple case of a statically quenched protein–fluorophore complex in equilibrium with a fully fluorescent state, for which changes in temperature should only alter the relative proportions of quenched and unquenched species present at excitation (Lakowicz, 1983). Associated decay times should remain unchanged.

In DHFR, a red shift of the absorbance maximum is observed in the difference spectrum of unbound versus bound NADPH with wtDHFR at higher temperatures; this shift reflects weakened interactions between the coenzyme carboxamide group and backbone of DHFR. The direction of the shift in wavelength toward lower energies does not parallel a decrease in observed fluorescence lifetimes of the excited state complex at elevated temperatures. That is, if ground state heterogeneity alone causes the observed variation in fluorescence decay rate for different mutants, decreased hydrogen bonding of wtDHFR to the carboxamide at higher temperatures might be expected to result in a longer fluorescence lifetime such as observed for mutant enzymes with absorbance maxima red-shifted relative to wtDHFR at 23 °C. However, more rapid fluorescence decay is observed at higher temperatures, consequently, we conclude that ground state heterogeneity in hydrogen bond contacts cannot explain the trend of decreased fluorescence lifetimes at elevated temperatures.

For most mutant DHFRs, the time course of fluorescence decay for NADPH is biphasic (with present resolution). Exceptions are the decay curves for NADPH bound to D27C and D27N which require several discrete components or a continuous distribution. Slow (nanosecond) dipolar relaxation resulting from a time-dependent relaxation of the protein matrix (tightly bound water molecules and amino acid side chains) could produce such a decay pattern with emission from unrelaxed states occurring at shorter wavelengths and earlier times compared to partially and fully relaxed states (Lakowicz, 1983). Yet, time-resolved spectra recorded at early, middle, and late time windows do not differ. Failure to observe a spectral shift during emission suggests that slow dynamic dipolar relaxation is not the cause of biphasicity. Invariant lifetimes for τ_2 at several wavelengths between 410 and 450 nm confirm the conclusion.

Dynamic Mechanisms of Fluorescence Decay. Two nonradiative decay mechanisms, internal conversion and collisional quenching, could produce the observed variation in fluorescence lifetime for NADPH in mutant holoenzyme complexes. In systems where the energy separation between $\pi\pi^*$ and $n\pi^*$ excited singlet states is small, radiationless transitions can proceed rapidly by internal conversion through the proximity effect (Lim, 1986). Nitrogen heterocycles containing carbonyl groups such as NADPH undergo electronic deexcitation when out-of-plane bending modes vibrationally couple to lower energy excited states. Even modest distortions in nuclear coordinates allow efficient coupling when the potential energy curves of $\pi\pi^*$ and $n\pi^*$ states overlap. Mixing of π–π^* transitions with n–π^* transitions leads to nonradiative return to the ground state. We use the term internal conversion in a broad sense here and do not imply anything about the spin labels of intermediate states.

The conclusion that enhanced rates of internal conversion occur for the holoenzyme of wild-type DHFR as compared with the mutants is supported by previous observations of different fluorescence decay times for sterically hindered dihydronicotinamides in solution. The fluorescence lifetime of *N,N*-dimethyl-1-(2,6-dichlorobenzyl)-1,4-dihydronicotinamide is considerably shorter than lifetimes of corresponding monomethylated and unmethylated derivatives (Fischer et al., 1988). In addition, vibrational bands in the second-derivative absorption spectrum of the monomethylated and unmethylated compounds are absent from the dimethylated amide spectrum. Wobbling of the $-N(CH_3)_2$ group was proposed to explain the

differences in lifetimes. Rapid movement of the amide group presumably increases the rate of nonradiative internal conversion by introducing out-of-plane bending modes for dissipating excited state energy through vibronic relaxation (Fischer et al., 1988).

Raman and resonance Raman experiments provide further evidence that changes in specific amide bending modes of the carboxamide group can affect the stability of the excited state of NADPH through coupling to ring stretching modes. Bowman and Spiro (1980) assigned the bands at 1616 and 1546 cm^{-1} to in-phase and out-of-phase C=C stretching modes of the nicotinamide ring. Due to its large intensity in resonance Raman spectra, they concluded that the 1546-cm^{-1} band must participate in the $\pi-\pi^*$ absorption transition of reduced nicotinamide. However, the 1546-cm^{-1} line often disappears from the Raman spectra of NAD(P) bound to dehydrogenases (Deng et al., 1989b). At the same time, the frequency of amide rocking modes changes from 1089 to 1113 cm^{-1}.[2] The coupling of amide rocking modes to dihydropyridine ring stretches is further suggested by an upward shift of the 1546-cm^{-1} band of NADPH upon deuteration of amide protons in D_2O (Bowman & Spiro, 1980; Yue et al., 1986). Callender and co-workers (Deng et al., 1989a) agree that coupling is likely to exist between carboxamide motions and dihydropyridine ring stretches of NADPH. Hence, it is reasonable to expect the extent of coupling between amide bending modes and dihydronicotinamide ring C=C stretches to affect radiationless decay of the excited state. Changes in binding the carboxamide of NADPH to mutant DHFRs should affect excited states and lead to changes in fluorescence lifetime.

Diffusion of quenchers to the chromophore during the lifetime of the excited state could also lead to decreased fluorescence lifetimes. In proteins, chromophores are often shielded from bulk solvent that can cause nonspecific quenching. Polar residues, such as carboxylic acids, amino groups, and sulfur-containing side chains may promote dynamic quenching, however, if they are located near sites of transition density in the excited state (Axelsen & Prendergast, 1989). If contact is made during the lifetime of the excited state, the excited state is rapidly deactivated. Dynamic quenching increases at higher temperatures because increased vibration amplitudes bring those side chains into closer contact with chromophores.

Since these two mechanisms share similar dependence on Brownian motion dynamics of the local environment, they are not easily distinguished experimentally.

X-ray Diffraction Results Suggest That a Mobile Loop Region between Residues 16 and 20 Could Be a Region of Dynamic Flexibility. A comparison of X-ray structures for binary $NADP^+$–DHFR with the ternary folate–$NADP^+$ complex suggests that a portion of the DHFR molecule, involving residues 15–20, encloses substrate and coenzyme in the ternary complex (Bystroff et al., 1990). This flexible Met20 loop is disordered along with the nicotinamide ring in the holoenzyme and, presumably, highly mobile in solution. In the ternary complex, dihydrofolate occupies a position above the coenzyme in the active site cleft with the pterin ring N5 nitrogen oriented toward C4 of the cofactor. As shown in Figure 5, the sulfur atom of methionine at position 20 is in van der Waals contact with the carboxamide amide group of NADP. The side chains of Asp27, Thr113, and Trp22 and water molecule 206 form a network of hydrogen-bonded groups which bind the pterin ring. This network appears to anchor the Met20 loop through an interaction of Asp27 and water 206 with Trp22. Another key contact stabilizing the Met20 loop in the complex is a hydrogen bond between the side chain of Asn-18 and the backbone of His45. This bridge between the Asn18 side chain and the His45 backbone restricts concerted movement of the Met20 loop and the ATP-ribose

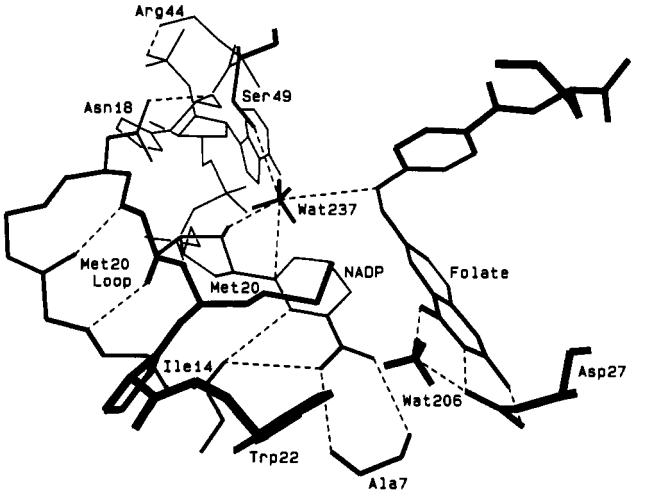

FIGURE 5: Top view of ternary folate–$NADP^+$ complex showing the Met20 loop and other key interactions of enzyme and substrate that afford stability to the closed form of the enzyme.

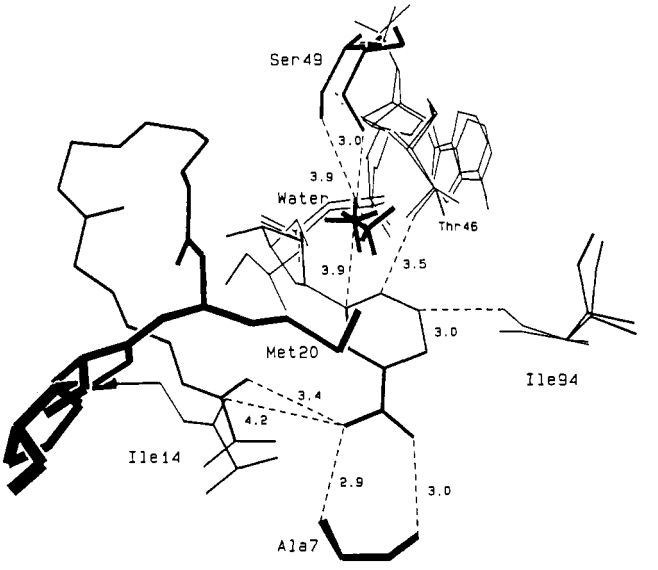

FIGURE 6: Overlay of structures for *E. coli* DHFR–$NADP^+$ and *E. coli* DHFR–$NADP^+$–folate complexes from X-ray data (Bystroff et al., 1990) showing possible displacement of the carbonyl oxygen of Ile14 from a hydrogen bond interaction with the carboxamide group of NADP. Not shown is the Met20 loop for the binary complex. This region is disordered in the crystal structure. The carbonyl group is visible and appears to be displaced relative to its position in the ternary complex. Although the change is small, it suggests that the location of carbonyl oxygen at position 14 is influenced by mobility of the Met20 loop.

[2] Lim (1986) states that "Since the out-of-plane modes active in the $n\pi^*-\pi\pi^*$ vibronic coupling have lower frequencies in the excited state than in the ground state (vide supra), these vibrations should be important accepting modes for radiationless decay of the lowest excited state. This conclusion becomes obvious when the anharmonicity associated with the active out-of-plane bending modes is included in the consideration of the Franck–Condon factors." The increase in amide rocking frequency from 1084 to 1114 cm^{-1} for unbound versus bound NADH (Deng et al., 1989b) suggests that hydrogen bond formations between enzymes and the carboxamide are stronger than comparable interactions in solution. However, with increased charge density developing in the carboxamide of bound NADPH in the excited state, hydrogen bonds to amide NH should be weaker. A downward shift in rocking frequency is expected. When this shift is maximal, greater vibronic coupling can occur between $n-\pi^*$ and $\pi-\pi^*$ transitions.

portion of bound coenzyme away from the enzyme surface. Further anchoring of the coenzyme is achieved through a strong electrostatic interaction between the 2′-phosphate group of NADPH and the guanidinium group of Arg44. Mutations that weaken these interactions on the enzyme could alter the equilibrium positions of the Met20 loop and the nicotinamide group of NADPH, or they could change the rate and amplitude of Met20 loop motions.

Possible Molecular Origins of the Proximity Effect and Dynamic Quenching in DHFR. Referring to Figure 6, movement of the Met20 loop should alter key molecular contacts between the protein environment and dihydronicotinamide ring. For example, a key interaction takes place between the carbonyl oxygen of Ile14 with the C2 of the nicotinamide ring (transition-state stabilization) and with the amide portion of the carboxamide. Perturbation of these interactions by mutations should affect activation of NADPH in the transition state during hydride transfer. A weak interaction with the carboxamide group would weaken all protein–nicotinamide interactions by allowing the nicotinamide ring to sample less favorable orientations within the cofactor binding pocket. At the same time, fluorescence lifetimes of bound coenzyme could increase because internal conversion rates decrease due to reduced overlap of excited states. Possible dynamic quenching of coenzyme fluorescence by the polarizable sulfur of Met20 would also depend upon exact positioning of the Met20 loop and its motion during the excited state lifetime. Contact must take place for quenching to occur (Lakowicz, 1983).

Model for Fluorescence Decay of NADPH Bound to DHFR. Our model for explaining fluorescence of dihydronicotinamide bound to DHFR involves two coenzyme conformations with different modes of excited state deactivation. One conformer has properties similar to dihydronicotinamide dissolved in aqueous solvents, namely rapid fluorescence decay and a red-shifted emission maximum. We do not expect this conformer to be identical to any species existing in solution, but from its lifetime, it is more like the short-lived species attributed to an "open" conformation. There could be some range of lifetimes and variety of conformations unresolved in present experiments. As suggested by recent X-ray diffraction results, the nicotinamide ring of bound $NADP^+$ can swing out toward solution when the Met20 loop adopts an open configuration (Bystroff et al., 1990). Such solvent exposed dihydronicotinamide would account for the (more or less) invariant decay times for the fast component of the biexponential fits. A more tightly bound species has a longer decay time that varies among different mutants of DHFR. In order to account for the variation in τ_2, we suggest that hydrogen bonds of variable strength between the carboxamide and different mutant enzymes produce variable rates of internal conversion by altering to different degrees wave function overlap between the initially excited $\pi\pi^*$ states and nearby $n\pi^*$ states. The change in frequency of the carboxamide amide rocking modes between ground and excited states is in the right direction to be active in the proximity effect (Lim, 1986). Additionally, dynamic quenching may be facilitated by nearby specific quenching groups of amino acid side chains such as the Met20 sulfur.

Longer decay times of NADPH in ternary complexes of *E. coli* with trimethoprim reflect the absence of excited state interactions between dihydronicotinamide and inhibitor in these complexes. A general blue shift in fluorescence wavelength maxima indicates a larger energy separation between the lowest excited state and the ground state. Medium-resolution X-ray diffraction data on the ternary complex of wild-type DHFR (Champness et al., 1986) place the trimethoxybenzyl side chain of TMP over the nicotinamide ring in the complex. One methoxy substituent appears close enough to be within van der Waals contact with the nicotinamide ring. If locating the Met20 loop close to the dihydronicotinamide ring facilitates nonradiative decay channels, trimethoprim may promote slower radiative decay by causing the Met20 loop to open away from the nicotinamide. The sulfur atom of Met20 would be displaced as a result of increasing van der Waals repulsion with TMP. Greater stability of electronically excited NADPH would occur in those mutant complexes in which the Met20 loop loosely closes over the active site. The larger energy separation between ground and excited states reduces overlap of potental energy surfaces in the excited state, thereby decreasing internal conversion. The human enzyme is different. There, the trimethoxybenzyl ring of TMP likely adopts an orientation similar to the (*p*-aminobenzyl)glutamate tail of bound folate, i.e., pointing away from the nicotinamide ring of NADPH, and the position of the flexible loop should remain unaffected by TMP while the nicotinamide ring is expected to be bound more tightly.

The differential effect of trimethoprim upon fluorescence lifetimes and CD spectra of NADPH bound to *E. coli* and vertebrate DHFRs warrants discussion. The appearance of an extrinsic Cotton effect near the nicotinamide absorption band in the CD spectrum of the ternary *E. coli*–TMP–NADPH complex is unexpected as no effect is observed in the spectrum of the binary complex. Equally puzzling is the reported (Hood et al., 1979) disappearance of rotational strength in the nicotinamide absorption for the *L. casei* (and presumably human DHFR) ternary complex since the binary complex showed a moderate Cotton effect at 350 nm. Fluorescence lifetime behavior is also different between NADPH bound to *E. coli* and human DHFRs. *Complexes exhibiting Cotton effects at 350 nm have longer fluorescence lifetimes for bound coenzyme.* The Cotton effects seen in CD spectra may reflect similar relative energies for the linear (π–π^*) and rotational (n–π^*) components (Hood et al., 1979). This degeneracy is observed in complexes where the environment surrounding the carboxamide presumably alters the degree of conjugation of the ring and carboxamide π systems. More separated transitions apparently occur in those enzyme complexes that not only have intact and strong hydrogen bonds between the carboxamide and protein backbone but also have a polarizable group, i.e., a sulfur atom, near the conjugated carbonyl group.

Correlation between Fluorescence Decay and Catalysis. The correlation between the rate of hydride transfer and the rate of decay of nicotinamide fluorescence in holoenzyme complexes of DHFR mutants possibly reflects movements of protein structure which directly influence both properties, albeit on quite different time scales. X-ray results reveal that the Met20 loop is a flexible region of DHFR. We have detailed possible implications for fluorescence quenching; these explanations all share the feature that altered fluctuating positions of the Met20 loop are responsible. That the Met20 loop is positioned near the nicotinamide and pterin binding sites suggests its importance. The major limb of the correlation in Figure 3, involving samples with fluorescence decay rates slower than wild-type DHFR, appears to follow a curve where logarithmic changes in catalysis occur for near-linear increases in fluorescence decay rate. Correlation of catalysis with the inverse sixth power of the fluorescence decay rate also describes the data. Such nonlinear relationships are typical of dipole-

induced dipole interactions in proteins (Fersht, 1985). The other, rapidly ascending limb of the graph, in which catalysis and fluorescence decay are not correlated, suggests that mutations can be made in DHFR that alter the rate of catalysis without perturbing the environment surrounding the coenzyme. In this study, mutations at position 27 which remove a critical component of the proton transfer mechanism greatly influence hydride transfer but have little impact on NADPH fluorescence. We infer that most mutations that principally perturb the binding of DHF should not influence the rate of fluorescence decay of bound NADPH, while most mutations that perturb the position of the Met20 loop will change the decay rate. Conversely, the data suggest that fluorescence decay parameters of mutant enzymes can be used to predict the influence of mutations upon the interactions within the cofactor binding site that stabilize the transition state of bound dihydronicotinamide.

How Might Flexibility in the Met20 Loop Affect Fluorescence and Catalysis? The position of the Met20 loop affects the location of the backbone carbonyl oxygen of Ile14 near the dihydropyridine ring and carboxamide of NADPH. This backbone carbonyl oxygen represents one of three conserved oxygen atoms which surround the dihydropyridine ring of bound coenzyme and promote partial positive charge development at the C4 of NADPH in the transition state through resonance stabilization (Figure 4). Removal or loss of the interaction between C2 of NADPH and the carbonyl group of Ile14 would result in decreased affinity of mutant DHFRs for the transition state. Not only would loss of the individual interaction between C2 of NADPH and the carbonyl oxygen of Ile14 destabilize the transition state, but all other stabilizing interactions may be perturbed as well because the nicotinamide ring could freely sample alternative orientations. Since these mutant DHFRs would not bind and recognize the transition state of reduced coenzyme as well, their catalytic potential is reduced.

Substitution of the amide group of NADPH with a methyl substituent in 3-acetylNADPH affects both fluorescence and catalysis. One might attribute the reduced rates of hydride transfer and longer fluorescence lifetime (τ_2 = 2.3 ns) of this analogue to its inability to participate in hydrogen bonding with the backbone carbonyl oxygen atoms of Ile14 and Ala7. The extended fluorescence lifetime for bound 3-acetylNADPH would result from either a reduced rate of internal conversion or reduced dynamic quenching in the excited state. Compared to NADPH, the analogue has a shorter intrinsic radiative half-life (Scott et al., 1970). The almost 2-fold greater increase in lifetime of 3-acetylNADPH relative to NADPH when bound to wtDHFR, therefore, implicates enzyme–carboxamide interactions in the fluorescence decay. In addition, neither wild-type DHFR nor mutant enzymes can efficiently stabilize partial charge deficiency in the pyridine ring of 3-acetylNADPH in the transition state because the weakened hydrogen bond interactions between the carbonyl oxygens of Ile14 and Ala7 and the coenzyme amide group lead to an overall loosening of the dihydropyridine ring of 3-acetylNADPH in the cofactor binding site and weakening of all protein–coenzyme interactions that stabilize the transition state.

An alternative explanation presumes a direct role of Met20 in catalysis. During enzyme turnover, the N5 of dihydrofolate receives a proton before or concomitant with hydride transfer to C6. Since the sulfur atom of Met20 is close to N5 of folate in the crystal structure of the ternary enzyme–folate–$NADP^+$ complex, Met20 may modulate the approach of solvent to N5 during catalysis. Transient fluctuations in the position of Met20 would momentarily affect the accessibility of N5 to solvent. Placing a hydrophobic group like Met20 near protonated N5 of dihydrofolate would be unfavorable and help shift the positive charge on nitrogen to the adjacent carbon, C6, thereby facilitating hydride addition (Bystroff et al., 1990). Mutant enzymes that have altered equilibrium or transient positions of Met20 may show less activity because they are unable to interact with or stabilize the activated form of protonated DHF. Changes in position of the Met20 loop alter the location of Met20 at the same time, and may alter the rate of hydride transfer accordingly.

Coupling of Protein Motions to Catalysis in DHFR. The question can be posed, "How can motions that contribute to decay of the excited state with a nanosecond fluorescence half-life also promote the rate of a catalytic step having a much slower rate constant near 1000 per second?" There has been some speculation. Dogonadze and Kuznetsov (1977) treat large conformational changes as a series of high-frequency oscillations coupled along the same reaction coordinate. Each productive oscillation gradually moves the system from some initial state to a different final configuration. Careri and Gratton (1986) emphasize the statistical nature of protein fluctuations; they estimate that conformational fluctuations with frequencies on the order of 10^9 s^{-1} should occur with sufficient probability, viz. 10^{-5}, to be active toward catalysis. The idea was that only relatively high-frequency conformational fluctuations could contribute to catalytic processes because slower motions would not occur with sufficient probability to influence reaction events.

Other authors suggest that specific low-frequency motions could contribute to catalysis as long as they are strongly coupled to the reactive event (Bialek & Onuchic, 1988). The concept of strong coupling between protein dynamics and catalysis suggests that specific protein modes modulate reaction rates in enzymes. The idea is that substrate binding can organize random conformational fluctuations in enzymes into specific modes that alter the population of reactive substrate molecules proceeding to the transition state.

Because the Met20 loop is a fairly large element of protein structure, Kramers's theory (Kramers, 1940) leads us to predict that the rate of hydride transfer will depend upon solvent viscosity if motion of the Met20 loop is coupled strongly to catalysis. Our failure to observe any substantial effect of glycerol upon the rate of hydride transfer argues against strong coupling of slow protein motions to catalysis in wtDHFR. A more likely mechanism for wtDHFR involves a non-rate-determining closure of the Met20 loop around the coenzyme and substrate within the ternary complex and a weak coupling of high frequency intramolecular modes to catalysis.[3]

Conclusions

Molecular motions in DHFR appear to influence the rate of fluorescence decay of NADPH in holoenzyme complexes. The proposed mechanism is the following: strong hydrogen bonding contacts between the coenzyme carboxamide and protein backbone in wtDHFR predispose bound dihydronicotinamide to efficient internal conversion or dynamic

[3] Reports of reduced magnitudes of deuterium isotope effects in the pre-steady-state reactions of several enzymes with mutations at position 44 (Adams et al., 1989) suggest that a conformational change in the ternary substrate complex may limit the rate of hydride transfer from reduced coenzymes to dihydrofolate. If movements of the Met20 loop have been disrupted by mutations at position 44, loop closure may become rate determining during the hydride transfer reaction; that is, loop motion has become strongly coupled to catalysis.

quenching. Very small structural changes affect the efficiency with which small-amplitude, high-frequency motions of the protein promote quenching. Arguments were presented against the alternative that the mechanism involves a purely static interaction affected by small structural changes. There is a possible correlation of these movements with other, slower, motions that enhance rates of hydride transfer from NADPH to dihydrofolate on the enzyme. One candidate for such motion is a fluctuation of the Met20 loop (see Figure 5). Movement of the loop could enhance stabilization of a putative electronic configuration of NADPH (Filman et al., 1982) in the transition state. Equally important, proper closure of the Met20 loop also compresses the distance between C4 of coenzyme and C6 of DHF in the transition state (Bystroff et al., 1990; Davies et al., 1990) and precisely defines a trajectory for hydride transfer. Transition-state compression is a recognized mechanism of reaction rate acceleration on enzyme surfaces. Mutations presumably affect the ability of enzymes to achieve an optimal distance between C4 and C6 for hydride transfer; for reasons not completely understood, nonradiative decay is reduced at the same time.

There are enzyme mutations that reduce hydride transfer but do not affect fluorescence decay, in particular, the series of mutant proteins containing amino acid substitutions at aspartic acid 27. All of these require preprotonated DHF for activity. Catalytic proficiency decreases in those enzymes primarily because the mutations have altered important interactions with DHF; coenzyme binding remains unperturbed for the most part, and consequently, coenzyme fluorescence is not disturbed. The Asp27 mutants of DHFR demonstrate that point mutations can be constructed that disturb the properties of only one of the two reactant surfaces. Conversely, the apparent correlation of fluorescence lifetimes with hydride transfer rates for other mutants indicates that other residues modulate both the catalytic and fluorescence behavior of bound coenzyme. Those mutations introduce effects localized to the Met20 loop or nicotinamide binding site.

Our attempt to document high-frequency motion is only a small step in unraveling the total picture. One may speculate that the catalytic step is coupled in various ways to motion on a wide range of time scales.

Acknowledgments

We thank Stephen Benkovic, Rick Wagner, Judith Klinman, and Gregory Farnum for their useful comments on preliminary versions of the manuscript; Murray Goodman for his discussion of CD spectroscopy; Cynthia David for providing samples of D27E and D27C DHFR; John Montgomery for his generous gift of 5-deazafolate; Katy Brown, Steve Dempsey, and Michelle McTigue for their help in constructing figures of DHFR; and Doug Tisdale, Forest Gompf, Dan Brewton, Robert Parker, and John Palmer for their technical assistance in modifying the Durrum and HI-TECH stopped-flow instruments.

References

Adams, J., Johnson, K., Matthews, R., & Benkovic, S. J. (1989) *Biochemistry 28*, 6611–6618.

Appleman, J. R., Howell, E. E., Kraut, J., & Blakley, R. L. (1990) *J. Biol. Chem. 265* (10), 5579–5584.

Axelsen, P. H., & Prendergast, F. G. (1989) *Biophys. J. 56*, 43–46.

Baumgarten, B., & Hones, J. (1988) *Photochem. Photobiol. 47*, 201–205.

Benkovic, S. J., Fierke, C. A., & Naylor, A. M. (1988) *Science 239*, 1105–1110.

Bialek, W., & Onuchic, J. N. (1988) *Proc. Natl. Acad. Sci. U.S.A. 85*, 5908–5912.

Birdsall, B., Burgen, S. V., & Roberts, G. C. K. (1980) *Biochemistry 19*, 3723–3731.

Birdsall, B., Feeney, G. C. K., Tendler, S. J., Hammond, D. J., & Roberts, G. C. K. (1989) *Biochemistry 28*, 2297–2305.

Bolin, J. T., Filman, D. J., Matthews, D. A., Hamlin, R. C., & Kraut, J. (1982) *J. Biol. Chem. 257*, 13650–13662.

Bowman, W. D., & Spiro, T. G. (1980) *J. Raman Spectrosc. 9*, 369–371.

Bystroff, C., Oatley, S. J., & Kraut, J. (1990) *Biochemistry 29*, 3723–3731.

Careri, G. (1974) in *Quantum Statistical Mechanics in the Natural Sciences* (Korsunoglu, B., Mintz, S. L., & Widmayer, S. M., Eds.) pp 15–34, Plenum, New York.

Careri, G., & Gratton, E. (1986) in *The Fluctuating Enzyme* (Welch, G. R., Ed.) pp 227–262, Wiley, New York.

Cha, Y., Murray, C. J., & Klinman, J. P. (1989) *Science 243*, 1325–1330.

Champness, J. N., Stammers, D. K., & Beddell, C. R. (1986) *FEBS Lett. 199*, 61–67.

Cocco, L., Roth, B., Temple, C., Montgomery, J. A., London, R. E., & Blakley, R. L. (1983) *Arch. Biochem. Biophys. 226*, 567–577.

Dauber-Osguthorpe, Roberts, V. A., Osguthorpe, D. J., Wolff, J., Genest, M., & Hagler, A. (1988) *Proteins: Struct., Funct., Genet. 4*, 31–47.

Davies, J. F., Delcamp, T. J., Prendergast, N. J., Ashford, V. A., Freisheim, J. H., & Kraut, J. (1990) *Biochemistry 29*, 9467–9479.

Deng, H., Zheng, J., Burgner, J., & Callender, R. (1989a) *J. Phys. Chem. 93*, 4710–4713.

Deng, H., Zheng, J., Sloan, D., Burgner, J., & Callender, R. (1989b) *Biochemistry 28*, 1525–1533.

Dogonadze, R. R., & Kuznetsov, A. M. (1977) *J. Theor. Biol. 69*, 239–263.

Evleth, E. M. (1967) *J. Am. Chem. Soc. 89*, 6445–6453.

Farnum, M. F., Magde, D., Hirai, J., Warren, M., David, C., Howell, E., Villafranca, J., & Kraut, J. (1990) *FASEB J. 4* (5).

Fersht, A. R. (1985) in *Enzyme Structure and Mechanism*, pp 293–299, Freeman and Company, New York.

Fierke, C. A., Johnson, K. A., & Benkovic, S. J. (1987) *Biochemistry 26*, 405–409.

Filman, D. J., Bolin, J. T., Matthews, D. A., & Kraut, J. (1982) *J. Biol. Chem. 257*, 13663–13672.

Fischer, P., Fleckstein, J., & Hones, J. (1988) *Photochem. Photobiol. 47*, 193–199.

Freisheim, J. H., & D'Souza, L. (1971) *Biochem. Biophys. Res. Commun. 45*, 803–808.

Greenfield, N. J. (1975) *Biochim. Biohysics. Acta 403*, 32–46.

Hood, K., & Roberts, G. C. K. (1978) *Biochem. J. 171*, 357–366.

Hood, K., Bayley, P. M., & Roberts, G. C. K. (1979) *Biochem. J. 177*, 425–432.

Howell, E. E., Villifranca, J. E., Warren, M. S., Oatley, S. J., & Kraut, J. (1986) *Science 231*, 1123–1128.

Howell, E. E., Warren, M. S., Booth, C. L., Villifranca, J. E., & Kraut, J. (1987) *Biochemistry 26*, 8591–8598.

Howell, E. E., Foster, P. G., & Foster, L. H. (1988) *J. Bacteriol. 170*, 3040–3045.

Karplus, M., & McCammon, J. M. (1983) *Annu. Rev. Biochem. 53*, 263–300.

Kramers, H. A. (1940) *Physica VII*, 283–304.

Kraut, J. (1988) *Science 242*, 534–560.
Lakowicz, J. R. (1983) in *Principles of Fluorescence Spectroscopy*, Plenum Press, New York.
Levitt, M., & Sharon, R. (1988) *Proc. Natl. Acad. Sci. U.S.A. 85*, 7557–7561.
London, R. E., Howell, E. E., Warren, M. S., Kraut, J., & Blakley, R. L. (1986) *Biochemistry 25*, 7229–7235.
Lim, E. C. (1986) *J. Phys. Chem. 90*, 6770–6777.
Magde, D., & Campbell, B. F. (1989) *Proc. SPIE 154, Fluorescence Detection III*, 61–68.
Maggiora, G., Johansen, H., & Ingraham, L. L. (1969) *Arch. Biochem. Biophys. 131*, 352.
Maharaj, G., Selinsky, B. S., Appleman, J. R., Perlman, London, R. E., & Blakley, R. L. (1990) *Biochemistry 29*, 4554–4560.
Matthews, D. A., Alden, R. A., Bolin, J. T., Freer, S. T., Hamlin, R., Xuong, N., Kraut, J., Poe, M., Williams, M., & Hoogsteen, K. (1977) *Science 197*, 452–455.
Matthews, D. A., Bolin, J. T., Burridge, J. M., Filman, D. J., Volz, K. W., Kaufner, B. T., Beddill, C. R., Champness, J. N., Stammers, D. K., & Kraut, J. (1985) *J. Biol. Chem. 260*, 381–391.
McCammon, J. A., Gelin, B. R., & Karplus, M. (1977) *Nature 267*, 585–590.
Morrison, J. F., & Stone, S. R. (1988) *Biochemistry 27*, 5499–5506.
Northrup, D. B. (1977) in *Isotope Effects in Enzyme Catalyzed Reactions* (Cleland, W. W., Ed.) University Park Press, Baltimore, MD.
Osaki, A. Y., King, R. W., & Carey, P. R. (1981) *Biochemistry 20*, 3219–3225.
Poe, M., Greenfield, N. J., Hirshfield, J. M., & Hoogsteen, K. (1974) *Cancer Biochem. Biophys. 1*, 7–11.
Rojas, G., & Magde, D. (1983) *Chem. Phys. Lett. 102*, 399–403.
Saperstein, D. D., Rein, A. J., Poe, M., & Leahy, M. F. (1978) *J. Am. Chem. Soc. 100*, 4296–4300.
Scott, T. G., Spencer, R. D., Leonard, N. J., & Weber, G. (1970) *J. Am. Chem. Soc. 92*, 687–695.
Searle, M. S., Forster, M. J., Birdsall, B., Roberts, G. C. K., Feeney, J., Cheung, H. T. A., Kompis, I., & Geddes, J. (1988) *Proc. Natl. Acad. Sci. U.S.A. 85*, 3787–3791.
Seng, G., & Bolard, J. (1983) *Biochimie 65*, 169–75.
Villafranca, J. E., Howell, E. E., Voet, D. H., Strobel, M. S., Ogden, R. C., Abelson, J. N., & Kraut, J. (1983) *Science 222*, 782–788.
Visser, A. J. W. G., & van Hoek, A. (1981) *Photochem. Photobiol. 47*, 201–205.
Waldman, A. D. B., Hart, K. W., Clarke, A. R., Wigley, D. B., Barstow, D. A., Atkinson, T., Chia, W. N., & Holbrook, J. J. (1988) *Biochem. Biophys. Res. Commun. 150*, 752–759.
Yue, K. T., Martin, C. L., Chen, D., Nelson, P., Sloan, D. L., & Callender, R. H. (1986) *Biochemistry 25*, 4941–4947.

Q-Band ENDOR Spectra of the Rieske Protein from *Rhodobactor capsulatus* Ubiquinol–Cytochrome *c* Oxidoreductase Show Two Histidines Coordinated to the [2Fe–2S] Cluster†

Ryszard J. Gurbiel,‡,§ Tomoko Ohnishi,*,‖ Dan E. Robertson,‖ Fevzi Daldal,⊥ and Brian M. Hoffman*,‡

Department of Chemistry, Northwestern University, Evanston, Illinois 60208, Institute of Molecular Biology, Jagiellonian University, Krakow, Poland, and Department of Biochemistry and Biophysics and Department of Biology, University of Pennsylvania, Philadelphia, Pennsylvania 19104

Received June 19, 1991; Revised Manuscript Received August 27, 1991

ABSTRACT: Electron nuclear double resonance (ENDOR) experiments were performed on ^{14}N (natural abundance) and ^{15}N-enriched iron–sulfur Rieske protein in the ubiquinol–cytochrome c_2 oxidoreductase from *Rhodobactor capsulatus*. The experiments proved that two distinct nitrogenous ligands, histidines, are undoubtedly ligated to the Rieske [2Fe–2S] center. The calculations of hyperfine tensors give values similar but not identical to those of the Rieske-type cluster in phthalate dioxygenase of *Pseudomonas cepacia* and suggest a slightly different geometry of the iron–sulfur cluster in the two proteins.

A protein containing a [2Fe–2S] iron–sulfur cluster and generally called the Rieske iron–sulfur protein was first isolated from the ubiquinol–cytochrome *c* oxidoreductase (cytochrome bc_1) of bovine heart mitochondria (Rieske, 1976). Its functional role as the primary electron acceptor of ubiquinol in the bc_1 complex, and as the electron donor to cytochrome c_1, is well accepted (Trumpower, 1981). Rieske iron–sulfur proteins have been found to be distributed in a variety of respiratory systems, such as the cytochrome bc_1 complex of photosynthetic and nonphotosynthetic bacteria (Bowyer et al., 1980; Meinhardt et al., 1987) and the cytochrome b_6f complex of chloroplasts and cyanobacteria. These cytochrome complexes contain two *b* hemes, one c_1 (or *f* in b_6f), and one Rieske iron–sulfur cluster. In all cases, the Rieske iron–sulfur cluster exhibits an EPR spectrum that is more anisotropic and

† This work was supported by NIH Grants HL 1353 (B.M.H.), GM 38237 (F.D.), and 27309 and by NSF Grants DMB 8907559 (B.M.H.) and DMB 8819305 (T.O.).
* To whom correspondence should be addressed.
‡ Northwestern University.
§ Jagiellonian University.
‖ Department of Biochemistry and Biophysics, University of Pennsylvania.
⊥ Department of Biology, University of Pennsylvania.

0006-2960/91/0430-11579$02.50/0